DOI: 10.24874/ti.2026.09.25.12

Tribology in Industry

www.tribology.rs

RESEARCH

Optimizing Solid Particle Erosion Wear Behaviour of the Flax Fiber Reinforced Epoxy Composites: Experimental Study Using RSM and ANFIS Approach

S.M. Vinu Kumar[a,*], N. Manikandaprabu[b], R. Hemanth[c], E. Sakthivelmurugan[d], N. Santhosh[e]

[a]*Department of Mechanical Engineering, Sri Krishna College of Engineering and Technology, Kuniyamuthur, Coimbatore, Tamil Nadu, India,*
[b]*Department of Electronics and Communication Engineering, Sri Krishna College of Engineering and Technology, Kuniyamuthur, Coimbatore, Tamil Nadu, India,*
[c]*Department of Mechanical Engineering, The National Institute of Engineering, Mysuru-570008, Karnataka, India,*
[d]*Department of Mechanical Engineering, Bannari Amman Institute of Technology, Sathyamangalam, Tamil Nadu, India,*
[e]*Department of Mechanical Engineering, Easwari Engineering College, Chennai, Tamil Nadu, India.*

Keywords:

Erosion efficiency
Flax fiber
Epoxy composites
Analysis of variance
Response surface method
Adaptive neuro-fuzzy inference system

* Corresponding author:

S.M. Vinu Kumar
E-mail: vinukmr1988@gmail.com

Received: 19 September 2025
Revised: 12 November 2025
Accepted: 4 December 2025

A B S T R A C T

Flax fiber reinforced epoxy (F-E) composites were prepared by hand layup technique followed by curing in compression moulding machine and were designated as 20F-E, 30F-E, and 40F-E, based on their fiber content. These laminates were subjected to solid particle erosion wear test in accordance with ASTM G76. With the help of Taguchi's design of experiments (L_{27} orthogonal arrays), tests were conducted for the different combinations of input parameters namely, impact velocities (72, 100, and 129 m/s), impingement angles (60, 75, and 90 degree), and fiber contents (20, 30, and 40 wt. %). Measured output responses of the study were erosion wear rate (EWR) and erosion efficiency (η). Results showed that the minimum EWR of 0.000165 g/g was observed for 40F-E composites under impact velocity 72 m/s, and impingement angle of 90°. Response surface methodology (RSM) and Adaptive Neuro-Fuzzy Inference System (ANFIS) models were developed for the EWR and their coefficient of determination (R^2) values were found to be 0.9827 and 0.9999, respectively. ANOVA reveals that impact velocity was the most significant factor influencing the EWR. Furthermore, validation test confirms that EWR of the ANFIS results were closer to experimental values than RSM model and hence proved its prediction accuracy. Worn damages like, crater formation, deep grooves, micro cutting, ploughing with partial deformations were predominant and exposed by field emission scanning electron microscope (FESEM).

1. INTRODUCTION

Natural fiber reinforced polymer composites (NFRPCs) are gaining acceptance over conventional synthetic fiber reinforced polymer composites due to biodegradability, light weight and cost-effectiveness [1-3]. With the ever-increasing ecological distress and the necessitate for sustainable engineering resolutions, natural strands such as hemp, sisal, coir, jute, etc., have been immensely explored in composite development for automotive, aerospace, biomedical and marine applications [4-8]. Among the numerous durability characteristics of NFRPCs, erosion wear, a progressive material loss due to continual collision of solid or liquid particles, particularly critical for parts that experiences high-velocity air or slurry jets [9,10]. The initial hypothetical fundamentals on erosion wear were placed by Finnie [11] and Bitter [12,13], who correlated the rate of wear to impact angle, velocity of the particle and material failure mechanisms. These models are benchmarks for present scenario as well. Further to their findings, several investigators explored the various combinations of the fillers and fibers in both thermoset and thermoplastic matrix, which clearly demonstrated that the erosion rate sturdily influenced by material constituents [14-16]. Arjula and Harsha [17] provided one of the foundational works on erosive wear of polymer composites by introducing the erosion efficiency (η) parameter to classify ductile, semi-ductile, and brittle responses under solid particle impact. They demonstrated that impingement angle and particle velocity are critical variables, with ductile polymers showing peak erosion at oblique angles (30°–45°) and brittle ones at normal impact (90°). This work established the theoretical framework for comparing polymer and composite erosion behaviour. On the other hand, the environmental concern, sustainability engineering agenda and remarkable report on lack of systematic study on natural fiber composites by Friedrich et al. [18] has diverted the researchers' attention towards the study of natural fibers reinforced polymer composites.

Gupta et al. [19] studied bamboo and other natural fiber composites, reporting that fiber content, length, and orientation strongly influence erosive wear. They showed that natural fibers tend to exhibit semi-ductile erosion behavior, with wear rates depending heavily on velocity and impingement angle, similar to synthetic fiber composites. Jena et al. [20] investigated bamboo/epoxy composites with cenosphere filler, reporting improved erosion resistance but poor performance in humid conditions. They highlighted that filler reinforcement enhances wear resistance by strengthening the fiber-matrix interface, but environmental degradation remains a limitation. Das and Biswas [21] studied coir/epoxy composites with and without Al_2O_3 filler, finding that unfilled composites exhibited maximum erosion at ~60° (semi-ductile), while filled composites shifted peak erosion to ~75° (semi-brittle) with lower wear rates. SEM analysis confirmed micro-ploughing, fiber thinning, and matrix cracking as key wear mechanisms. Manjunath et al. [22] reported that incorporation of nanofillers in natural fiber composites significantly enhanced erosive wear resistance. Improved fiber–matrix interfacial bonding was the primary mechanism for better performance. This work emphasized the potential of nanoscale modifications to overcome inherent weaknesses of natural fibers. Nayak and Mohanty [23] investigated areca sheath fiber reinforced PVA composites, observing semi-ductile erosion behavior with maximum wear at 45°. Optimum fiber content (10–27 wt. %) provided best erosion resistance. Chemical treatments (alkali, benzoyl chloride) improved fiber-matrix adhesion, reducing wear rates. Sahu and Gupta [24] made an effort of developing newer surface modification method on sisal fibers (untreated, treated with $NaHCO_3$, and treated with $NaHCO_3$ along with PLA coating) reinforced epoxy composites. They investigated the erosive wear behaviour of the epoxy-sisal composites. They revealed that the maximum wear resistance was offered by the treated and coated fibers reinforced composites than pure sisal fiber reinforced composite at 60° impact angle. Sangilimuthukumar et al. [25] investigated the erosive wear behaviour of jute, kenaf, banana fiber reinforced epoxy hybrid composites. They revealed that the erosion rate of hybrid composites increased with the increase in exposure time and maximum erosion rate was observed at 60° impingement angle. Boggarapu

et al. [26] reviewed and reported the works of various researchers on erosion wear behaviour of various polymer matrix composites. They emphasized to conduct research to develop theoretical models in estimating erosion wear rate and its dependency on micro-structure of constituents in the composite. Johnson et al. [27] investigated the erosion behaviour of NaOH treated and untreated sansevieria cylindrica (with varying fiber content and fiber length) reinforced vinyl ester composites. They implemented the Taguchi design of experiments to determine the optimum erosive wear parameters. They reported that the lowest wear loss parameters as the NaOH treated fiber of length 30 mm with 40 wt. % fiber content, impingement angle 90˚, impact velocity 41 m s^{-1}, erodent discharge 4 g min^{-1} and an exposure time of 15 min. Verma et. al [28] investigated the erosive wear behaviour of dolomite filled natural (grewia optiva)-synthetic (glass) fiber reinforced epoxy composites. They incorporated the Taguchi design of experiments to determine the optimal erosive wear parameters. They reported the lowest wear rate of the epoxy composites with the presence of 10 wt. % dolomite, 30˚ impingement angle, 10 m s^{-1} impact velocity and 150 μm sized erodent. Erosion resistance of red mud filled/unfilled sisal fiber reinforced polyester hybrid composites was studied by Vigneshwaran et al. [29]. They demonstrated the prominent parameters influencing maximum erosion loss as erodent velocity, red mud content in the composite and erodent discharge by implementing Taguchi design of experiments. Presence of red mud in the polyester composite demonstrated better resistance to erosion wear. Further, they observed that the maximum erosion rate at lower impact angle and with increasing erodent velocity. Premkumar et al. [30] investigated the erosion wear responses of polyester composites reinforced with NaOH treated and untreated curaua fiber. They implemented the design of experiments and revealed that the erodent impingement angle played a pivotal role in controlling the erosion rate of the composite. Antil et al. [31] optimized erosive wear response of fiber-reinforced epoxy composites using Taguchi methods and genetic algorithms (GA). Results indicated that impingement angle (~63 %) and reinforcement size (~28 %) were the most influential parameters. This work demonstrated the utility of statistical optimization techniques in wear studies. These traditional approaches have helped to identify dominant parameters, but they often struggle to capture nonlinear relationships and multi-factor interactions that govern wear behaviour. Machine learning (ML) techniques blended with statistical tools to analyse and predict the erosion wear behaviour of epoxy composites was reported by Mahapatra and Satapathy [32]. Test schedule was prepared based on the design of experiments. They implemented the analysis of variance to identify the significant factors and their contribution for wear rate. They reported that the most significant factor as impact velocity (81.2 %), followed by impingement angle (13.56 %), erodent temperature (0.06 %) and stand-off distance (0.05 %). Further, support vector machine, decision tree, random forest and gradient boosting machine (GBM) algorithms were used under ML approach to predict the erosion performance of the epoxy composites. The performances of four different ML models are compared on the basis of their coefficient of determination (R^2 value). It is found that the GBM outperforms other models with R^2 = 0.9543 and has emerged as the best-performing prediction model.

From the literature survey it is evident that much of the work on erosive wear behaviour of flax fiber reinforced epoxy composites and prediction of wear performances using fuzzy inference techniques are scarce. Hence to understand and identify the erosive wear significant factors, their contributions and to predict the erosive wear performance of the flax fiber reinforced epoxy composites, this investigation has been undertaken.

2. EXPERIMENTAL DETAILS

2.1 Material used

Flax fiber offers better mechanical strength and stiffness. Moreover, it is lesser dense than synthetic fibers and processing is easier. Thus, flax fibers were chosen as reinforcement member in to the epoxy matrix. Flax fiber yarns were procured from local vendors and weaved into irregular-basket woven architecture using handloom machine (Make: ERGO G2). Aerial

density of the flax fabric was found to be around 578 g m^{-2} and its schematic configuration is illustrated in the Fig. 1. Epoxy matrix was employed as a matrix material as it exhibits better adhesion, lower shrinkage and possess superior mechanical stability. By reinforcing the flax woven fabric with epoxy matrix, overall performance of the natural fiber composites can be enhanced by properly adjusting their weight fraction composition. Epoxy matrix was supplied by the Vasavibala Resins Pvt. Ltd., Chennai, India. Physico-chemical properties of the epoxy resin, hardener and flax fiber is shown in the Table 1.

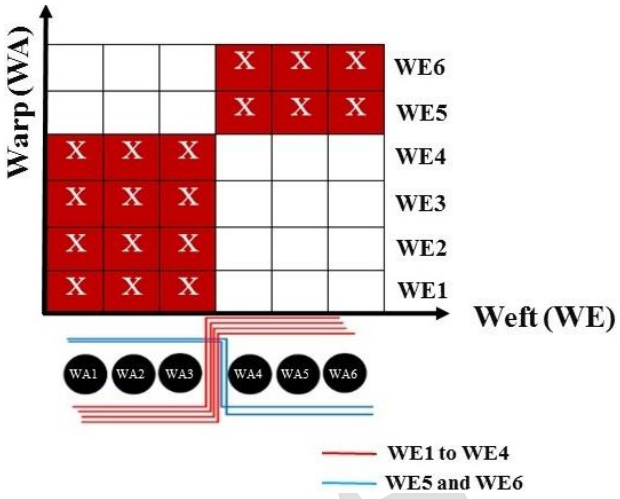

Fig. 1. Architecture of the flax woven fabric [2].

Table 1. Physical and chemical properties of the epoxy, hardener and fiber [2].

S. No	Raw Material	Grade	Characteristics
1	Epoxy grade	VBR8912	• Appearance-Mild yellow clear viscous liquid. • Viscosity at 25°C: 12730 mPa. S. • Density at 25°C :1.16 g/cc. • Epoxy value: 5.34 Eq/Kg. • Gel time: 69 min.
2	Epoxy hardener	VBR1209	• Appearance- Pale yellowish clear liquid. • Viscosity at 25°C: 453 mPa. S. • Density at 25°C: 0.98 g/cc. • Epoxy value: 5.34 Eq/Kg. • Refractive index at 25°C: 1.45-1.48
3	Flax Fiber	-	• Average diameter: 5-38 µm • Density: 1.5 g/cc • Cellulose: 71 (wt. %) • Hemicelluloses: 18.6-20.6 (wt. %) • Lignin: 2.2 (wt. %) • Wax: 1.7 (wt. %) • Pectin: 2.3 (wt. %) • Moisture content: 8-12 (wt. %) • Microfibrillar angle: 5-10 Degree • Tensile Strength: 345- 1035 MPa • Modulus: 27.6 GPa • Elongation: 2.7- 3.2 %

2.2 Fabrication of Flax fiber reinforced epoxy (F-E) composites

Flax fiber reinforced epoxy (F-E) composites were prepared using traditional hand layup process as it offers several advantages like, simple requirements, lower cost, and ease of modification. Initially, know weight fraction of the flax woven fabric was measured and to that, appropriate epoxy resin and its hardener mixture with proper ratio was prepared, as per the supplier recommendation. In the next step, a layer of flax fabric was placed on bottom mould which was made of mild steel, over which resin mixture was applied and spread throughout the fabric using brush and metallic roller. This step was repeated until all required layers of flax woven fabric was laid one above the other. These laminas consisting of epoxy resin mixture at their interface are compressed by means of closing the top and bottom mould. Finally, entire mould was compressed in a temperature-controlled compression moulding machine at a pressure range 15 to 17 bar at room temperature over a period of 24 hours. After successful curing of flax/epoxy laminates, it was removed from the mould and used for the erosion wear study as per

the ASTM standard. In this way, different composition of the F-E composite having, 20, 30 and 40 wt. % of fiber reinforcement was prepared, and so designated as 20F-E, 30F-E, and 40F-E respectively. Steps for preparing the F-E composites are illustrated in the Fig .2.

Fig. 2. Steps followed in the preparation of F-E composites.

2.3 Erosion wear test

Erosion wear test was conducted in an Air jet erosion test rig as per ASTM G76 standard [14-16] and its schematic representation is shown in the Fig. 3, indicating major components like high pressure heater, erodent nozzle, mixing chamber, and nozzle system. F-E composite samples were prepared to the dimension of 25 mm × 25 mm × 5 mm. Test was performed at a constant mass flow rate of erodent 3.3 g min^{-1}, for various impact velocities (72, 100, and 129 m s^{-1}) and impingement angles (60°, 75° and 90°).

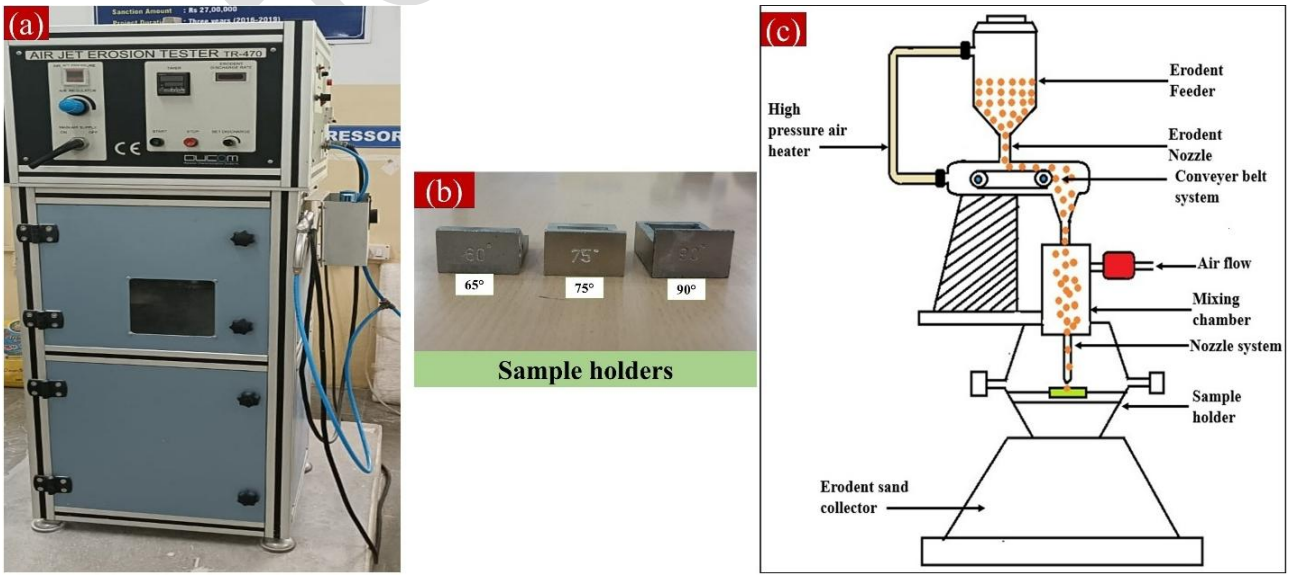

Fig. 3. Experimental set up of air jet erosion test rig.

Nozzle of diameter 1.5 mm was utilized, which directs and accelerates the erodent particles to strike the target surface. Stand-off distance was the distance between nozzle exit and work surface and was kept constant throughout the study which was maintained at 10 mm. Alumina particles of size 20-30 μm used as an erodent. Surface morphology of the solid particles was captured using scanning electron microscopy (SEM) and elemental composition using energy dispersive spectroscopy (EDS) which is displayed in the Fig. 4a and 4b. Worn surfaces were examined using Field Emission Scanning Electron Microscope (FESEM).

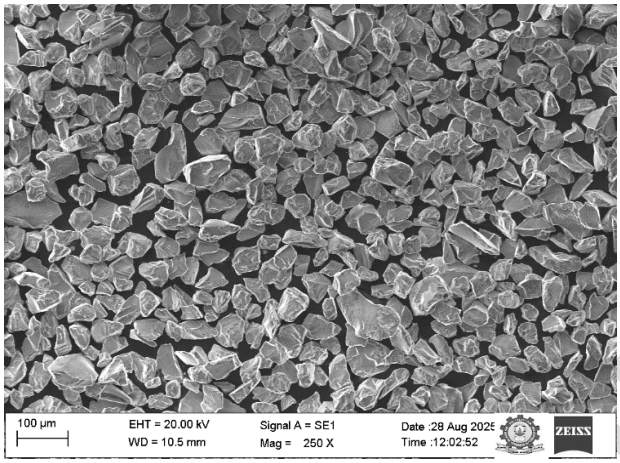

Fig. 4a. SEM picture of dry alumina particles.

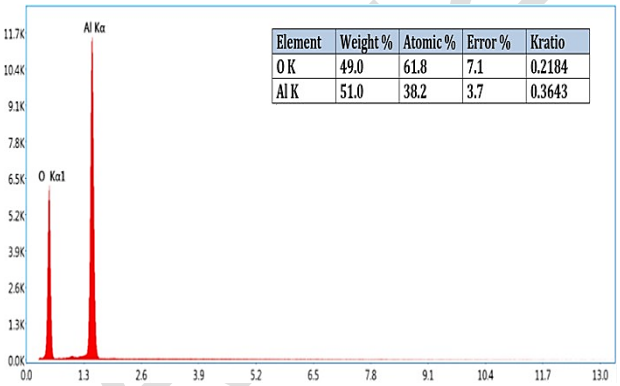

Element	Weight %	Atomic %	Error %	Kratio
O K	49.0	61.8	7.1	0.2184
Al K	51.0	38.2	3.7	0.3643

Fig. 4b. EDS result of dry alumina particles.

The weight of the F-E samples was carefully noted before and after the erosion to compute the actual mass loss of the sample using electronic balance (accuracy ±0.001). Erosion test samples of F-E composites before and after the erosion wear is presented in the Fig. 5a and Fig. 5b, respectively. The erosion wear rate (EWR) was calculated by employing equation (1)

$$EWR = \frac{\Delta w}{\Delta w_e} \quad (1)$$

where Δw and Δw_e represents the moss loss of the F-E sample (in grams) and mass of the eroding particles, respectively. Δw_e was further determined by including the testing time and feed rate of the solid particles. The erosion efficiency (η) of the eroded F-E samples was found using the following equation (2).

$$\text{Erosion efficiency } (\eta) = \frac{2 \times EWR \times H_r}{\rho\, v^2} \quad (2)$$

where EWR represents erosion wear rate (g/g), H_r is the hardness of the eroding sample (Pa), ρ and v are the actual density of the F-E sample (kg m^{-3}) and striking or impact velocity of the solid particles (m s^{-1}), respectively.

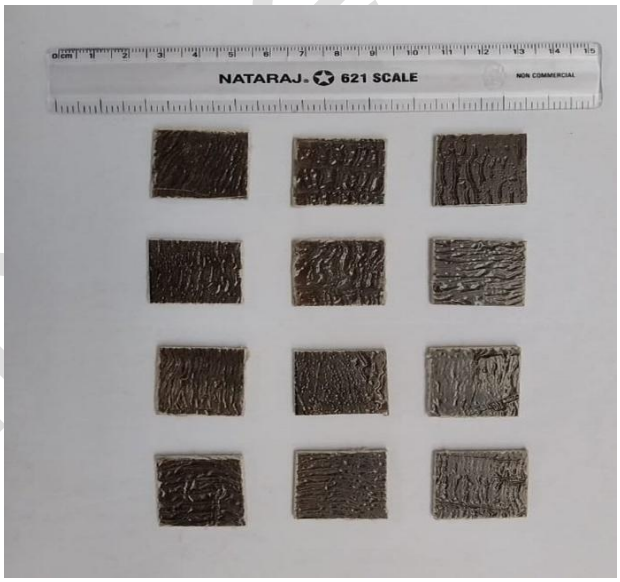

Fig. 5a. F-E composite samples before erosion wear.

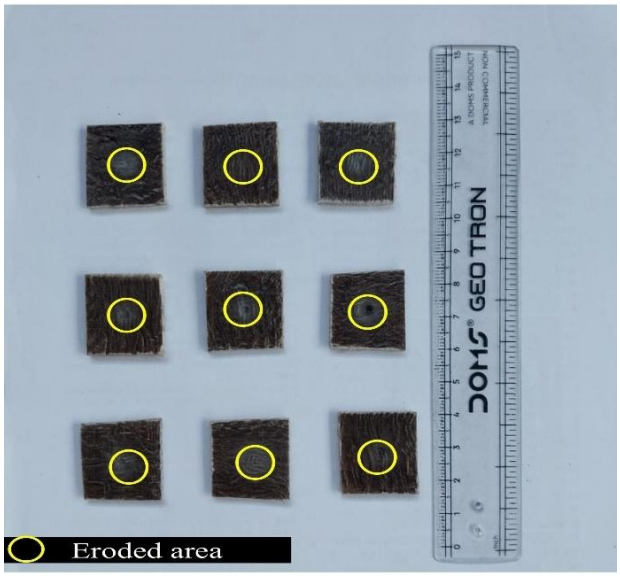

Fig. 5b. F-E composite samples after erosion wear.

2.4 Design of experiments

The main reason for applying the Taguchi's orthogonal arrays is that, it can effectively analyse the complete process parameters by conducting only few sets of experiments for the selected input functions. Taguchi design of experiments (TDoE) serves in avoiding repetitive tests thereby by saves times, materials and eventually testing costs. As experiments are mainly trusted on the input factors, all possible combination of the functions is experimentally explored. TDoE approach has a reputation of giving different levels of parametric combinations for the better performance of the process. TDoE involves collects of data, data analysis and data interpretation in order to meet the objective of the process. This is achieved by performing the experiments for the different levels of the input parameters as suggested in the design layouts. Therefore, selection of the input parameters plays a crucial as it strongly effect the performance of the study. In this present investigation, Taguchi's orthogonal array L_{27} was selected for three input factors namely, Impingement angle, impact velocity and fiber content and each of their three levels are shown in the Table 2. Three trails were conducted for each test and average was reported for final analysis. Main factors responsible for EWR of the F-E composites were analyzed.

Table 2. Input factors and their levels.

Symbol	Input Factors	Levels			Units
		I	II	III	
A	Impact velocity	72	100	129	(m s^{-1})
B	Impingement angle	60	75	90	(Degree)
C	Fiber content	20	30	40	(wt. %)

2.5 Response surface methodology and adaptive neuro-fuzzy inference system

Primary objective of any manufacturing process is to produce high quality products with minimal effort. For achieving such an endeavor, numerous experimental trails are required which is time-consuming and expensive. To overcome such burdens, it is mandated to adopt a pre-planned experimental design that integrates systematic data analysis for seamless process. Therefore, application of statistical tools not only helps in support of planning and conducting experiments, but also in analyzing the experimental results by limiting errors. Although there are several statistical-modeling techniques are available, present investigation emphases on Response Surface Methodology (RSM) and Adaptive Neuro-Fuzzy Inference System (ANFIS) and their respective models are developed using Design Expert and MATLAB software. RSM in mainly intended to establish the relationships between input parameters and to investigate the effect of process variables on selected response, in this case, erosion wear rate (EWR). Moreover, RSM enables in developing the quantitative correlations among input parameters and response variables, and thereby facilitates detailed analysis of their interdependencies. The relationship between the control input parameters of erosion wear of F-E composites and the response is shown in the equation (3).

$$f_u = \psi\left(y_{1u}, y_{2u}, y_{3u}, \ldots . y_{ku}\right) + \varepsilon_u \qquad (3)$$

where $u=1,2,3,\ldots k$ and k represents factorial experiment number. y_{iu} denotes the level of the ith factor in the u^{th} experiment. The function ψ is called the response surface. The residual ε_u measures the experimental error in corresponding u^{th} observation. The second order polynomial equation, that is, quadratic response surface has two variables and is given in the equation (4)

$$f_u = \beta_0 + \beta_1 y_{1u} + \beta_2 y_{2u} + \beta_{11} y_{1u}^2 + \beta_{22} y_{2u}^2 + \beta_{12} y_{1u} y_{2u} + \varepsilon_u \qquad (4)$$

where, $\beta_0, \beta_1, \beta_2$ ..... are the regression coefficients of the input variable (y).

The quadratic model indicated in the equation (4) is created for expecting the approximation of output variable by the values received through experiments. Further its efficacy is validated by ANOVA. Finally, model fitness is checked by the coefficient of determination (R^2) value.

Adaptive Neuro-Fuzzy Inference System (ANFIS) is widely known for integration of neural networks with fuzzy logic principles. Due to its hybrid learning tactics combined with a multilayered feed forward network, ANFIS proved to be quite faster and achieves rapid learning and convergence. ANFIS has several interconnected layers of nodes which effectively involved in exchange of the information via

direction links and further system errors are reduced by adjusting the input functions. Input factors are indicated as membership functions (MFs). These MFs helps in linking the input factors with output response variables. There are several MFs, in this study, generalized bell-shaped (gbellmf), Gaussian (gaussmf), and two-parameter Gaussian (gauss2mf) membership functions are employed. Based on the input parameters, training is performed at various iteration levels and based on which 27 fuzzy rules are generated. Table 3 shows the ANFIS parameters and types of membership function used in the erosion wear analysis of F-E composites. There are two main fuzzy inference systems namely, Mamdani FIS and Sugeno FIS. In the present study Sugeno approach is used and its operating principle and architecture is shown in the Fig. 6, and Fig. 7, respectively. Validation of the erosion parameters involved in Sugeno FIS is illustrated in the Fig. 8. Finally, performance or effectiveness of the ANFIS model is determined by root mean square error (RMSE) and mean absolute error (MAE), computed using equations (6) and (7), respectively. These metrics helps in measuring the accuracy of the predicted response against the experimental results.

$$RMSE = \sqrt{\frac{\sum(j-k)^2}{m}} \quad (6)$$

$$MAE = \frac{\sum|j-k|}{m} \quad (7)$$

where, m, j and k are number of patterns, set of actual and predicted output, respectively.

Coefficient of determination (R^2) is determined for understanding the effectiveness of the mathematical model used and its value generally ranges from 0 to 1. Equation (5) is used for calculating the R^2 value, which gives insight on the relationship between one term's performance and its prediction on the performance of another term.

$$R^2 = 1 - \frac{\sum(j-k)^2}{\sum(j-\bar{k})^2} \quad (5)$$

where $\bar{k}$ s the mean of the predicted output. The accuracy of the performance factors calculated is in 10^{-10}. The model with minimum average checking error is preferred, which gives good results.

Table 3. ANFIS information of membership function of F-E composites during erosion wear test.

Sl. No	Parameters	Membership functions		
		gbellmf	gaussmf	gauss2mf
1	Number of nodes	78	78	78
2	Linear	27	27	27
3	Non-linear	27	24	27
4	Total number of parameters	54	51	54
5	Number of fuzzy rules	27	27	27

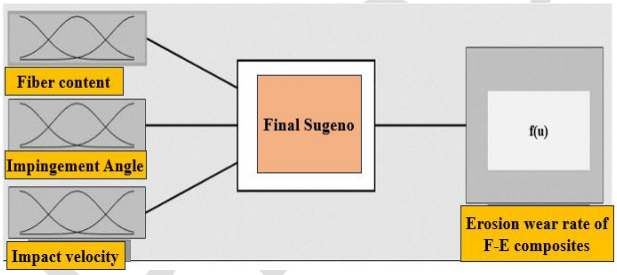

Fig. 6. Sugeno model with input functions used in erosion wear test of F-E composites.

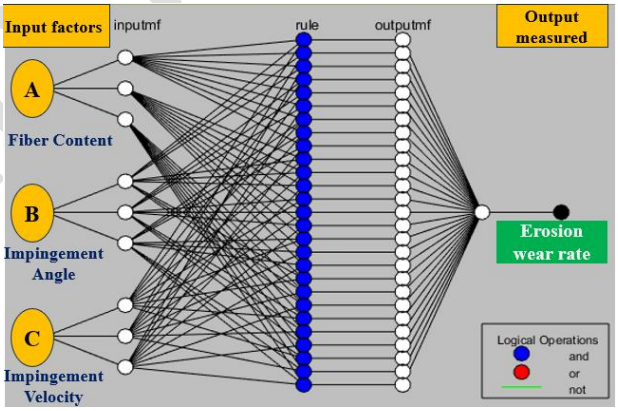

Fig. 7. ANFIS architecture employed for erosion wear test of F-E composites.

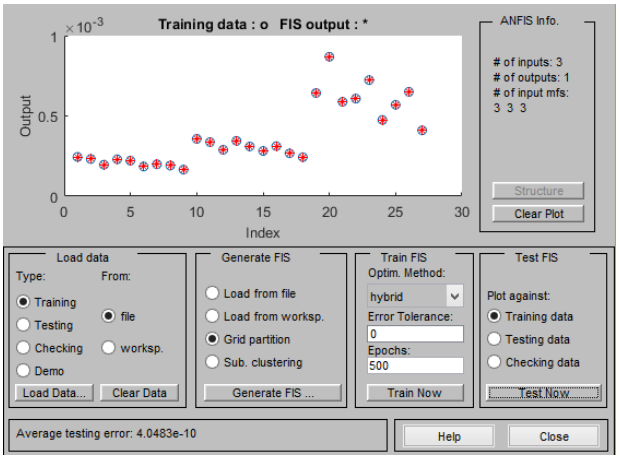

Fig. 8. Validation of input parameter (erosion wear) with Sugeno model in MATLAB (R2017a).

3. RESULTS AND DISCUSSION

Figures 9a-c shows the variation of the EWR of the different composition of F-E composites with respect to an impingement angle at which erodent particles strike the composite surface. It is evident from the plot that increase in the fiber content in F-E composite has improved the erosion wear rate (EWR) property. It means EWR value decreases with increases in the fiber content, indicating better resistance to erosion wear. Amongst the F-E composites, 40F-E showed the better EWR. This may be due to the higher hardness property of the composites since harder material resist the indentation and cutting action of the erodent particles, unlike soft materials. Furthermore, higher weight fraction of fiber content supports for the lower exposure of the epoxy-matrix as fiber act as a barrier thereby reduces plastic deformation and micro-cutting significantly.

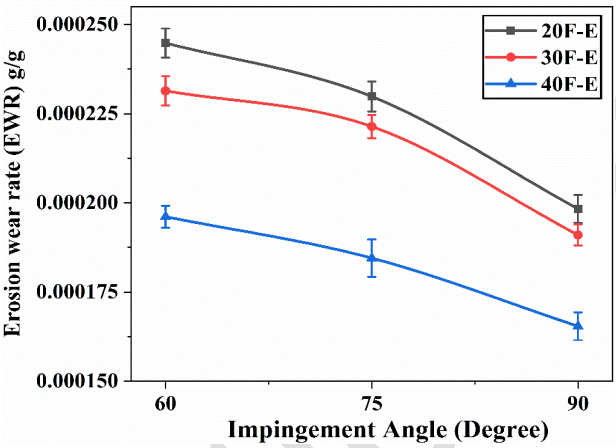

Fig. 9a. EWR of F-E composites at different impingement angles at a constant impact velocity of 72 m s^{-1}.

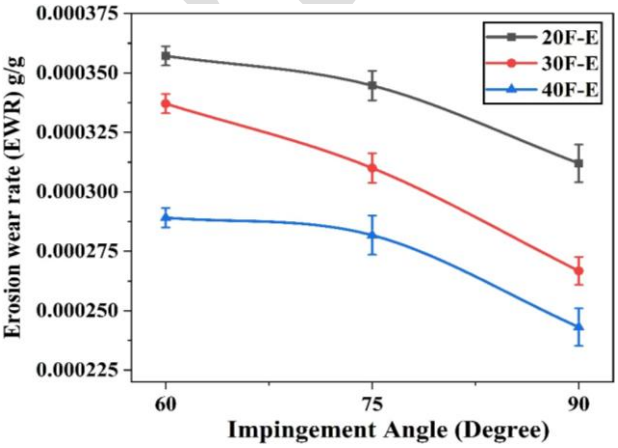

Fig. 9b. EWR of F-E composites at different impingement angles at a constant impact velocity of 100 m s^{-1}.

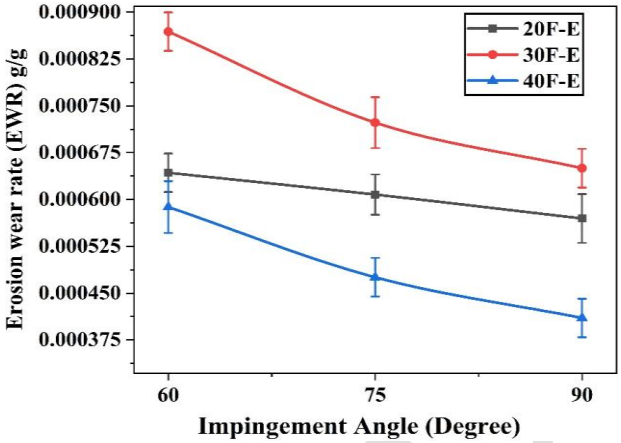

Fig. 9c. EWR of F-E composites at different impingement angles at a constant impact velocity of 129 m s^{-1}.

Table 4. Erosion test results of the F-E composites.

Trial No	Levels of factors			EWR (g/g)	Erosion efficiency (%)
	A	B	C		
1	72	60	20	0.00024480	3.5320
2	72	60	30	0.00023140	3.4530
3	72	60	40	0.00019610	2.8400
4	72	75	20	0.00022980	3.3150
5	72	75	30	0.00022140	3.3040
6	72	75	40	0.00018450	2.6720
7	72	90	20	0.00019830	2.8610
8	72	90	30	0.00019100	2.8500
9	72	90	40	0.00016540	2.3950
10	100	60	20	0.00035720	2.6710
11	100	60	30	0.00033710	2.6080
12	100	60	40	0.00028915	2.1710
13	100	75	20	0.00034470	2.5780
14	100	75	30	0.00031000	2.3980
15	100	75	40	0.00028175	2.1150
16	100	90	20	0.00031200	2.3330
17	100	90	30	0.00026675	2.0630
18	100	90	40	0.00024310	1.8250
19	129	60	20	0.00064274	2.8890
20	129	60	30	0.00086882	4.0390
21	129	60	40	0.00058791	2.6520
22	129	75	20	0.00060790	2.7320
23	129	75	30	0.00072309	3.3610
24	129	75	40	0.00047542	2.1450
25	129	90	20	0.00056960	2.5600
26	129	90	30	0.00065011	3.0220
27	129	90	40	0.00041021	1.8510

From the Figs. 9a-c it can be further noted that, EWR decreases with increase in the impingement angle regardless of the impact velocity at which erodent particles striking with. Impingement angle plays a crucial role in determining the behaviour of the composite material. According

to sharma and kumar et al. [33] whether the eroded material is brittle or ductile can be judged by correlating the EWR values against the impingement angle. For ductile materials, EWR is maximum at an impingement angle range 15-30°, whereas for brittle material at higher striking angle (90°). However, in the present case maximum EWR is found at an impingement angle 60°, which is clearly an evident of the semi-ductile material and it is consistent with the reported literatures [33-36]. When the erodent particle striking at an oblique angle causes intense shearing action with normal stress. These dual actions combining leads to fiber-matrix debonding and micro-fracture and so higher EWR. As impingement angle increases to normal 90°, drastic reduction of EWR is noted in all F-E composites. This may be owing to the less shearing action but impact of normal striking is dominated by compression and this resulting lesser material removal and hence lowers EWR in flax/epoxy composites [37,38]. Further it can be noticed that increase in the impact velocity has increased the EWR as indicted in the figure 9. This may be owing to the combined effect of increased particle turbulence and momentum. The significant increase in momentum has paved the way for effective conversion of kinetic energy into work done in terms of removal of material. Moreover, erodent striking at higher velocity causes severe plastic deformation and occurrence of fatigue phenomena is inevitable and thus resulted in higher EWR. This discussion is consistent with the previous reports [33,39].

Figures 10a-c shows the EWR of the F-E composites with respect to impact velocities for different impingement angles. It is evident from the plot that, increase in the fiber content in the F-E composites imparted the better resistance property to the erosion wear. Amongst the fabricated F-E lots, 40F-E laminate showed least EWR under all conditions. This may due to the fact that, higher content of fiber (40F-E) strengthens the epoxy matrix, and thus paves for more absorption of impact energy across the distributed fibers instead of causing material removal. Moreover, at lower velocities, erodent particles rather than causing deep cutting gets deflected due to the presence of fibers by absorbing impact energy and so erosion wear decreases. But increases in the velocity from 100 m s^{-1} to 120 m s^{-1}, significant rise in the EWR is observed and the trend remained same for the erodent particles striking at different impingement angle. Increased in the impact velocities of the erodent particles increases the kinetic energy which is sufficient enough to cause intense cutting, and micro-ploughing due to the repeated and continuous impact of erodent particles on the F-E surface. Thus, more materials are eroded owing to the severe micro-cracking and cutting, debonding of fiber-matrix region, and surface fatigue, resulting in higher accelerated erosion wear [40]. Furthermore, interfacial bonding between flax fiber and epoxy matrix also plays a vital role in assessing the erosion wear behavior of the F-E composites. From the plot it is evident that, 40F-E exhibited lower EWR, this may be owing to better bonding at higher fiber loading, which makes quite difficult for the erodent particles to dislodge the surface of the material, causing lower erosion wear. In case of the 30F-E composites, EWR is quite higher than the 20F-E, but lower to 40F-E composite. At this intermediate level of fiber loading, F-E composite likely to have possessed the balanced matrix dominated and fiber dominated properties. When the erodent particle impacts the 30F-E surface, it tries to resist for some extent. Since fiber-matrix bonding is not as strong as 40F-E composites, preventing of fiber pullouts or debonding is quite challenging and inevitable. Thus, EWR is higher at intermediate fiber loaded 30F-E composites compared to higher fiber 40F-E composites. Furthermore, it is interesting to note that, 30F-E composite exhibited higher EWR than 20F-E when erodent particle striking at 120 m s^{-1}. This may be attributed to the fiber fragmentation process, as flax fiber tends to break or split under the influence of repeated higher energy impact, eventually resulting in more erosion wear loss.

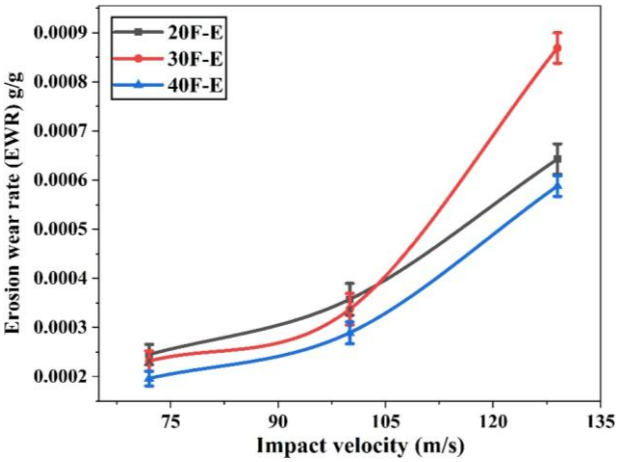

Fig. 10a. EWR of F-E composites at different impact velocities at a constant impingement angle of 60°.

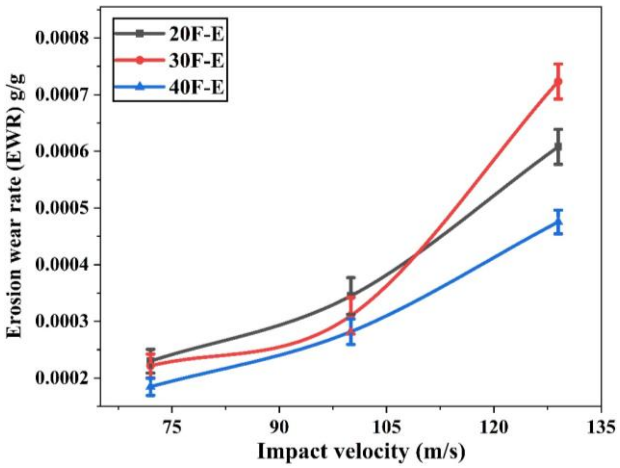

Fig. 10b. EWR of F-E composites at different impact velocities at a constant impingement angle of 75˚.

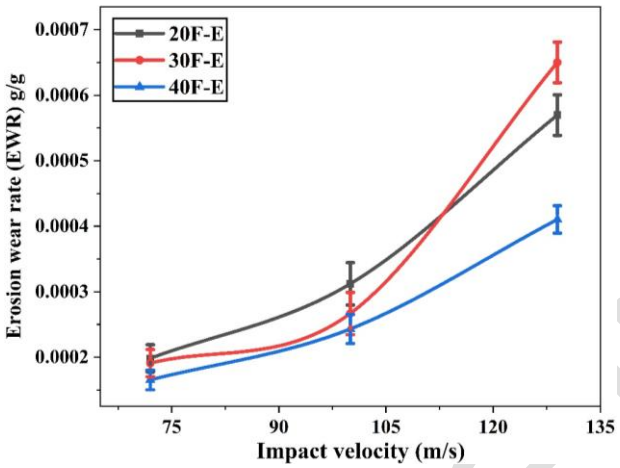

Fig. 10c. EWR of F-E composites at different impact velocities at a constant impingement angle of 90˚.

It was reported earlier studies [41,42] that the impact velocity of the abrasive particles has a strong influence of the EWR. Relation between EWR and impact velocity is established using power law equation [8]:

$$EWR=Kv^{n} \quad (8)$$

Where, "EWR" is the Erosion wear rate, "v" is the impact velocity of the abrasive particles, "n" and "K" are the velocity exponent and constant, respectively. The least-square fits to data points were achieved by employing equation (8) and fitting parameters at different impingement angles for the F-E composites are indicated in the Table 5.

From the Table 5 it is evident that velocity exponents "n" values found in the range of 1.63 to 2.2, typically closer to 2.0 for the F-E composite at different impingement angles. As mentioned earlier that erosion behaviour of the F-E composite materials is broadly classified as ductile and brittle based on the impingement angle. However, this may not absolute as the erosion behaviour depends on various factors such as, impact velocity, impact angle, shape and size of the abrasive particles, abrasive flow rate, and stand-off distance and etc. Mohanty et al. [41] reported that erosion characteristics of the polymer-based composite is highly relied in the velocity component "n". If the polymer composite material behaving in a ductile manner, then "n" value in the range of 2 to 3 whereas for brittle materials in the range 3 to 5. However, in the present investigation velocity exponent "n" is in the range 1.63 to 2.2, so F-E composite demonstrates semi-ductile behaviour and it is consistent with our previous discussion.

Table 5. Parameters characterizing the velocity dependence of EWR of the F-E composites.

Impingement angle (Degree)	Type of Composite	K	n	R^2
60	20F-E	2×10^{-7}	1.6317	0.9665
	30F-E	2×10^{-8}	2.2156	0.9341
	40F-E	7×10^{-8}	1.8496	0.9546
75	20F-E	2×10^{-7}	1.6477	0.9745
	30F-E	4×10^{-8}	1.9821	0.9303
	40F-E	2×10^{-7}	1.6041	0.9835
90	20F-E	9×10^{-8}	1.7896	0.9791
	30F-E	3×10^{-8}	2.0497	0.9271
	40F-E	2×10^{-7}	1.5393	0.9697

The effect of striking velocity and angle of impact on erosion wear behavior of the F-E composite can be comprehended by erosion efficiency (η) as illustrated in the Figures 11a-c and Figure 12a-c. It helps in understanding the mode of failure whether ductile or brittle characteristics [40]. It also acts as indicator conveying effectiveness in transforming kinetic energy of erodent particles into material removal [43]. From the plots it is evident that, η value varies from 1.82% to 4.03%. This range of erosion efficiency clearly indicate the semi-ductile behavior of the erosion which further supplement to our earlier claim. Pradhan and Acharya et al. [43] investigated the erosion wear behavior of Eulaliopsis binate (EB) fiber reinforced epoxy composite. They reported η values in the range 3.09 % to 9.2%, and claimed semi-ductile wear behaviour. Similar trend in erosion efficiency was reported for wood particulate filled epoxy composites by Prakash et al. [44].

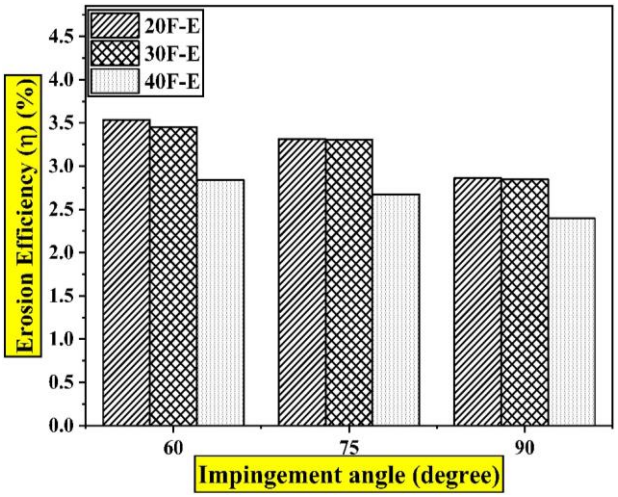

Fig. 11a. Erosion efficiency (η) of F-E composites as a function of impingement angle at an impact velocity 72 m s^{-1}.

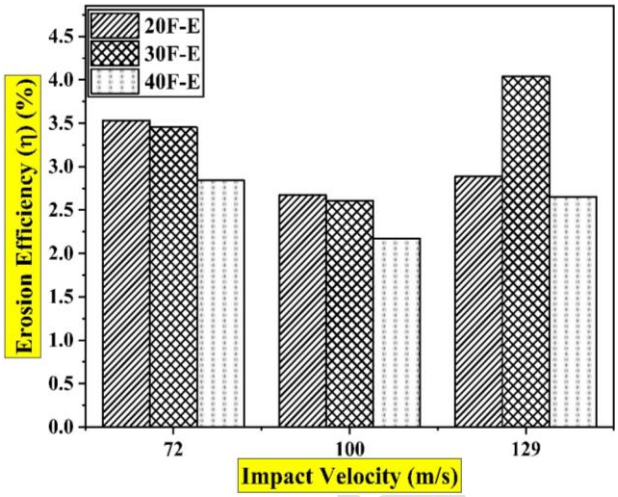

Fig. 12a. Erosion efficiency (n) of F-E composites as a function of impact velocity at an impingement angle 60˚.

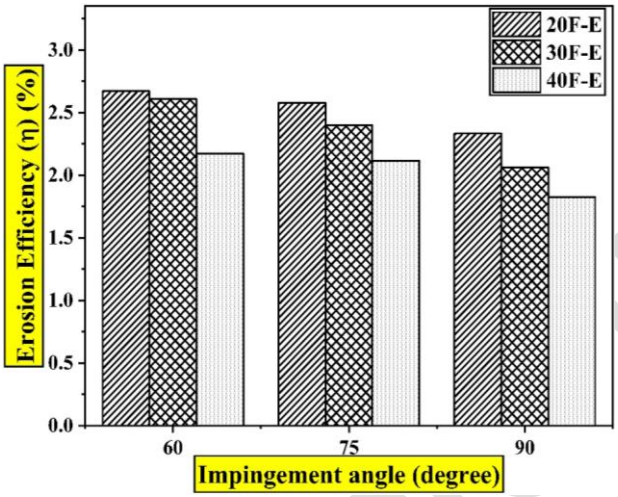

Fig. 11b. Erosion efficiency (η) of F-E composites as a function of impingement angle at an impact velocity 100 m s^{-1}.

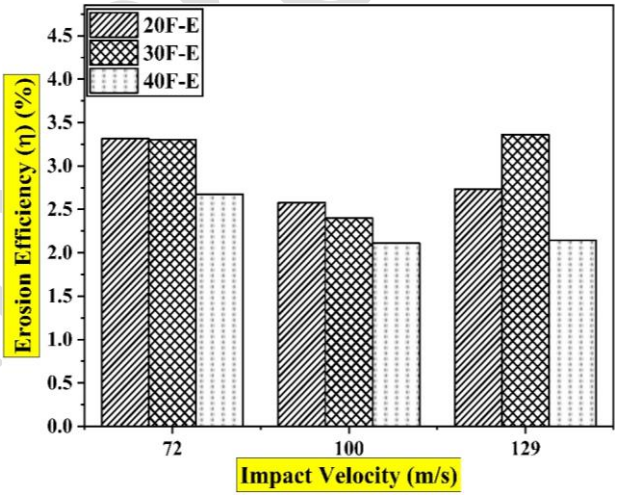

Fig. 12b. Erosion efficiency (n) of F-E composites as a function of impact velocity at an impingement angle 75˚.

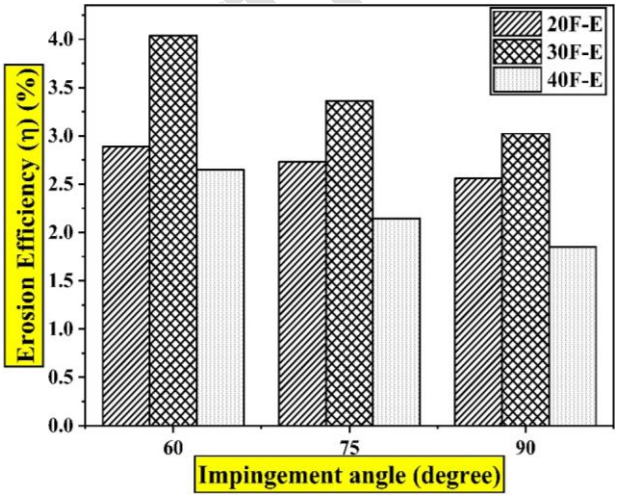

Fig. 11c. Erosion efficiency (η) of F-E composites as a function of impingement angle at an impact velocity 129 m s^{-1}.

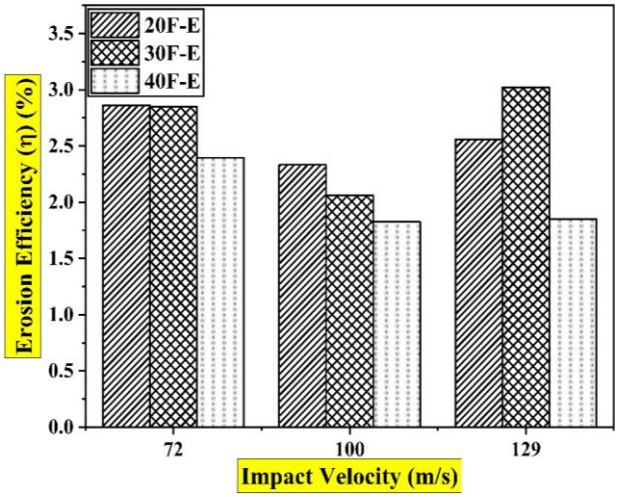

Fig. 12c. Erosion efficiency (n) of F-E composites as a function of impact velocity at an impingement angle 90˚.

Fiber reinforced polymer composites are being widely used in the aerospace, automotive, and construction sectors where they are exposed to harsh weathering conditions, particularly few applications where these composite materials have to deal with erosive environments. Therefore, understanding of the erosion behavior before placing in to actual working environment is necessary to predict the service life and reliability. In this present investigation as per Taguchi's orthogonal arrays L_{27} considering three input factors namely, fiber content, impingement angle and impact velocity which is varied at three levels and response variable erosion wear rate of the F-E composites are detailed in Table 4. This allows identifying the optimization of input parameters for better erosive wear resistance without sacrificing strength to weight advantages. From the Table 4 it is evident that EWR of the F-E composites obtained in the range 0.0001654 g/g to 0.00086822 g/g and found to be increased with increase in the impact velocity of particles and decreased with increase in impingement angle. However, increased in the fiber content in F-E composite has improved the resistance to erosion wear this may be attributed to strong interfacial adhesion between fiber-matrix which strictly restricts the displacement of composite material by erosion particles. Thus, it can be inferred erosion wear rate for the developed F-E composites will be less when erosion particles impact at lower velocity at higher impinging angle, especially for higher loaded F-E composites. Table 6 shows the comparison of the EWR of the F-E composites with other types of polymer composite.

Experimental findings revealed that all three input parameters at their different combinations have a significant impact on the erosion wear rate of the F-E composites. It is clear that erosion wear rate of F-E composites can be lower when erodent particles striking at higher impingement angle and lower velocity. Thus, lower EWR considerably arrest the fiber-matrix debonding, surface roughness, micro cutting and micro-cracking. This eventually favors the F-E composites to retain strength, and fatigue resistance over the period of time.

Experimental values of EWR were utilized to generate the RSM and ANFIS models for analyzing their prediction ability and further to state the better modeling approach. Moreover, Analysis of variance (ANOVA) is employed to assess the input factors significantly affecting the EWR and so parametric combination responsible for minimizing of the EWR can also studied. Thus, it supports in decision making and optimization of experimental findings in a statistical manner. Following RSM models namely, linear, cubic, 2FI, and quadratic are studied to understand their effectiveness in prediction of output response EWR. Table 7 shows the summary of the RSM model employed in analysis of erosion behavior of the F-E composites. It is evident that cubic model with R^2 value 0.9827 found to be superior than other three models and its regression model is shown in the Table 8.

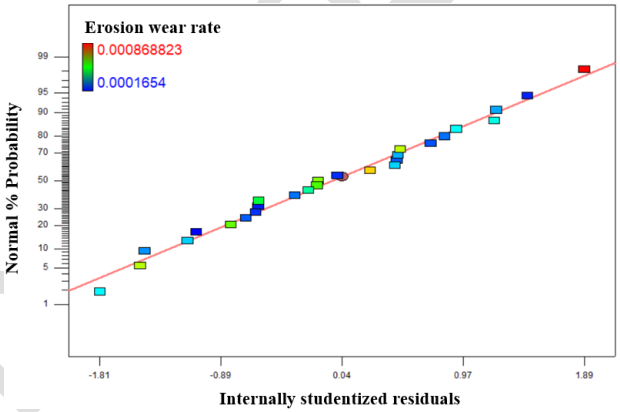

Fig. 13. Normal probability graph of the erosion wear test performed on F-E composites.

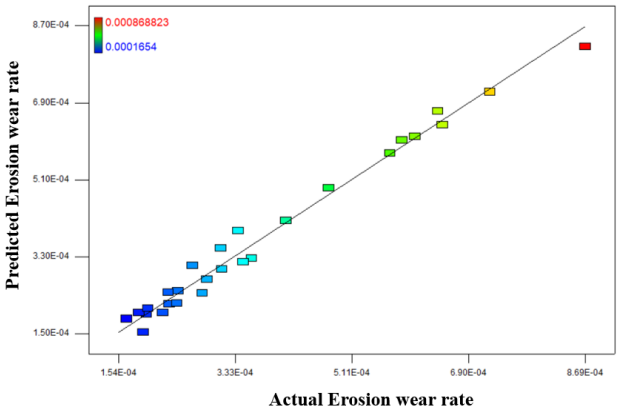

Fig. 14. Predicted and actual erosion wear rate of the F-E composites.

Normal probability plot and correlation of actual and predicted plot of EWR are presented in the Fig. 13 and Fig. 14, respectively. It is clearly noted from the plot that EWR values are found to be distributed normally and anticipated EWR values are closer to the practical ones and thus cubic RSM model comparatively found to be beneficial than other three.

Table 6. Comparison of the EWR of the F-E composites with other polymer composites.

S. No	Composites	Erosion parameters	EWR (g/g)	Erosion efficiency	Reference
1	Linz- Donawith sludge filled Polypropylene composites	• Impact velocity: 32 m/s to 64 m/s • Impingement angle: 30° to 90° • Erodent size: 50 to 250 microns • Temperature: 30 to 70	0.00003035 g/g to 0.00007732 g/g	-	14
2	Linz - Donawitz sludge (LD sludge), blast furnace slag (BF slag) and Linz - Donawitz slag (LD slag) Filled epoxy composites	• Impact velocity: 32 m/s to 64 m/s • Impingement angle: 30° to 90° • Erodent size: 50 to 250 microns • Temperature: 30 to 70	0.00004215 g/g to 0.00007135 g/g	-	15
3	Coconut shell dust filled epoxy composites	• Impact velocity: 100 m/s to 300 m/s • Impingement angle: 45° to 90° • Erodent size: 300 to 500 microns • SOD: 10 mm to 20 mm • Temperature: 30 to 70	0.00001728 g/g to 0.0001291 g/g and 0.00005825 g/g to 0.00015665 g/g	-	16
4	Bi-directional bamboo reinforced epoxy composites	• Impact velocity: 30 m/s, 52 m/s & 60 m/s. • Impingement angle: 30° to 90° • Erodent size: 125 to 300 microns • SOD: 10 mm • Feed rate: 4.7 g/min	0.0005 g/g to 0.0078 g/g	-	19
5	Cenosphere filled bamboo fiber reinforced epoxy composites	• Impact velocity: 33 m/s, 48 m/s & 70 m/s. • Impingement angle: 30° to 90° • Erodent size: 200 microns • SOD: 10 mm • Feed rate: 10 g/min	0.000095 g/g to 0.00145 g/g	2 to 22%	20
6	Alumina filled Coir/epoxy composites	• Impact velocity: 48 m/s, 70 m/s, 82 m/s and 109 m/s • Impingement angle: 30° to 90° • Erodent size: 200 microns • SOD: 10 mm • Feed rate: 2.5 to 3 g/min	0.000074 g/g to 0.00178 g/g	-	21
7	Areca sheath (AS) fiber reinforced polyvinyl alcohol (PVA) composites	• Impact velocity: 48 m/s, 70 m/s, 82 m/s and 109 m/s • Impingement angle: 30° to 90° • Erodent size: 200 microns • SOD: 10 mm • Feed rate: 1.45 g/min	0.00011 g/g 0.00387 g/g	0.652 to 14.882%	23
8	$NaHCO_3$ and PLA coated sisal/epoxy composites	• Impact velocity: 31.58 m/s, 52.94 m/s, 75 m/s and 100 m/s • Impingement angle: 30° to 90° • Erodent size: 50 microns • SOD: 10 mm • Feed rate: 1.45 g/min	0.00011 g/g 0.00168 g/g	-	24
9	Sansevieria cylindrica reinforced vinylester composite	• Impact velocity: 41 m/s, 72 m/s and 100 m/s • Impingement angle: 30° to 90° • Feed rate: 2.5 to 4.0 g/min	0.0000725 g/g to 0.000376 g/g	-	27
10	Redmud filled sisal fiber reinforced polyester composites	• Impact velocity: 42 m/s, 75 m/s and 100 m/s • Impingement angle: 30° to 90° • Erodent size: 50 microns • Feed rate: 2.5 to 4.0 g/min	0.000052 g/g to 0.000292 g/g	-	29
11	Pistachio shell particles filled kenaf/glass fiber reinforced polyester hybrid composites	• Impact velocity: 42 m/s, 75 m/s and 100 m/s • Impingement angle: 30° to 90° • Erodent size: 200 microns • Feed rate: 2.5 to 4.0 g/min	0.00125 g/g to 0.0042 g/g	5.9% to 32.9 %	40
12	Eulaliopsis binata fiber epoxy composite	• Impact velocity: 48 m/s, 72 m/s, 82 m/s and 116 m/s • Impingement angle: 30° to 90° • Erodent size: 200 microns • Feed rate: 3 g/min	0.000024 g/g to 0.00032 g/g	3.09 % to 9.20 %	43

13	Flax fiber reinforced epoxy composites	• Impact velocity: 48 m/s, 70 m/s, 82 m/s and 109 m/ • Impingement angle: 30° to 90° • Erodent size: 20-30 microns • Feed rate: 4 g/min	0.000165 g/g to 0.000868 g/g	1.82 % to 4.03 %	Present study

Table 7. Summary of the RSM models.

Source	Standard deviation	R^2	Adjusted R^2	Predicted R^2	PRESS
Linear	8.5005E-005	0.8270	0.8074	0.7699	2.248E-007
Cubic	4.1101E-005	0.9827	0.9550	0.8833	**1.148E-007(suggested)**
2FI	8.8696E-005	0.8451	0.7987	0.7439	2.501E-007
Quadratic	5.866E-005	0.9410	0.9084	0.8495	1.471E-007

Table 8. RSM model of EWR for cubic model.

Response	Model expression	R^2
Erosion wear rate (g/g)	3.550E-004+ (2.578E-004)×A - (4.075E-005)×B - (3.634E-005)×C - (2.933E-005)×AB - (1.832E-005)×AC - (7.557E-006)×BC + (1.028E-004)×A^2 + (3.325E-007)×B^2 - (7.048E-005)×C^2 - (1.511E-005)×ABC - (2.149E-005)A^2B - (5.830E-006)×A^2C + (1.351E-005)×AB^2 - (9.407E-005)×AC^2 + (4.056E-006)×B^2C + (1.997E-005)×BC^2	98.27%

Table 9. Information of ANFIS model chosen for erosion wear rate of F-E composites.

Model parameters	Membership functions		
Chosen membership function	gbellmf	gaussmf	gauss2mf
No. of Epochs	500	500	500
Error (%)	4.0483×10^{-10}	4.0916×10^{-10}	4.0651×10^{-10}

Table 10. ANOVA for the erosion wear rate in F-E composites.

Source	Sum of Squares	DF	Mean Square	F-value	p-value
Regression Model	9.599E-007	16	5.999E-008	35.50	< 0.0001 (significant)
A	2.392E-007	1	2.392E-007	141.56	< 0.0001
B	5.976E-009	1	5.976E-009	3.54	0.0894
C	4.752E-009	1	4.752E-009	2.81	0.1245
AB	1.032E-008	1	1.032E-008	6.11	0.0330
AC	4.026E-009	1	4.026E-009	2.38	0.1537
BC	6.852E-010	1	6.852E-010	0.41	0.5386
A^2	6.341E-008	1	6.341E-008	37.53	0.0001
B^2	6.633E-013	1	6.633E-013	3.925E-004	0.9846
C^2	2.980E-008	1	2.980E-008	17.64	0.0018
ABC	1.826E-009	1	1.826E-009	1.08	0.3230
A^2B	1.846E-009	1	1.846E-009	1.09	0.3206
A^2C	1.359E-010	1	1.359E-010	0.080	0.7825
AB^2	7.305E-010	1	7.305E-010	0.43	0.5257
AC^2	3.540E-008	1	3.540E-008	20.95	0.0010
B^2C	6.581E-011	1	6.581E-011	0.039	0.8475
BC^2	1.595E-009	1	1.595E-009	0.94	0.3542
Residual	1.690E-008	10	1.690E-009		
Cor Total	9.768E-007	26			

The RSM plots of EWR for the different combinations of input variables for eroded F-E composites are presented in the Fig. 15a-c. From the RSM plots it is evident that, EWR in F-E composites is completely governed by a balance of selected input variables. It is understood that increase in the striking velocity of the particles increases the EWR in F-E composites. At higher velocity severe damages such as fiber fracture and fiber-matrix debonding are predominant which is supplement to the semi-ductile nature of failure as EWR maximum at 60° impingement angle. However, increases in the fiber loading can strengthen F-E composites against the erosion attack and furthermore performing erosion tests for the higher fiber loaded composites at higher impingement angles and under lower velocities can significantly reduce erosion wear.

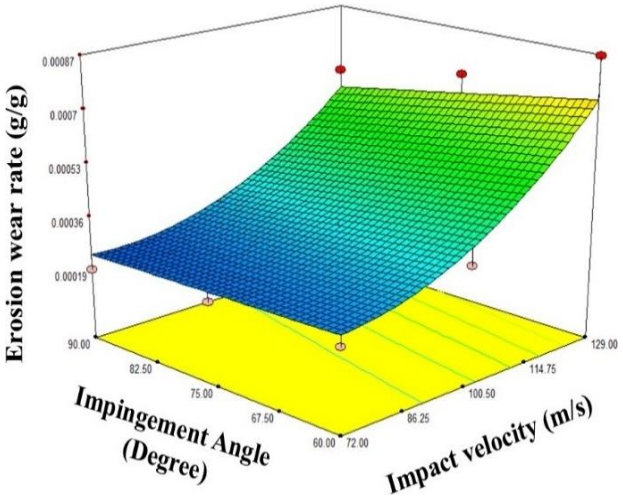

Fig 15a. RSM plot for the response erosion wear rate of F-E composites as a function of impingement angle and impact velocity.

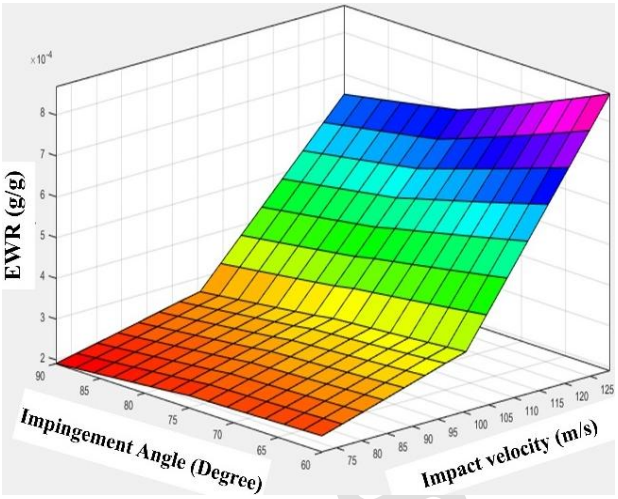

Fig 16a. ANFIS plot for the response erosion wear rate of F-E composites as a function of impingement angle and impact velocity.

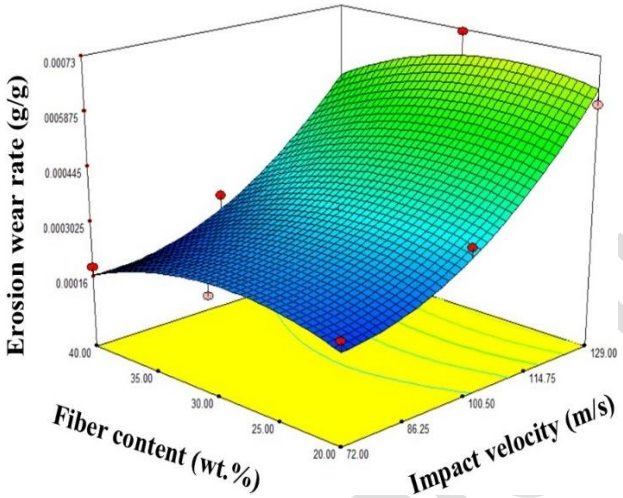

Fig 15b. RSM plot for the response erosion wear rate of F-E composites as a function of fiber content and impact velocity.

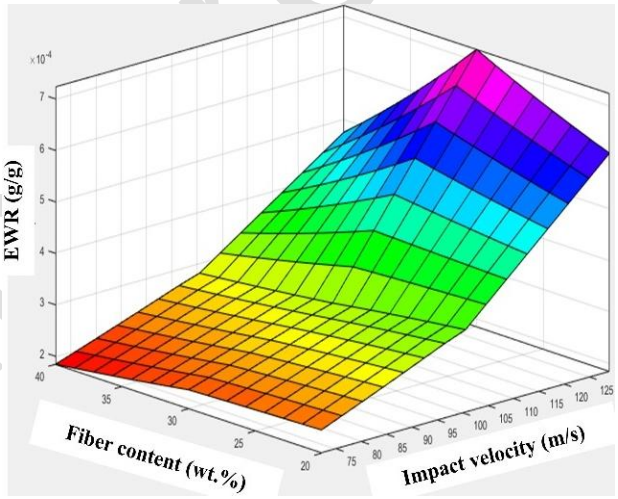

Fig 16b. ANFIS plot for the response erosion wear rate of F-E composites as a function of fiber content and impact velocity.

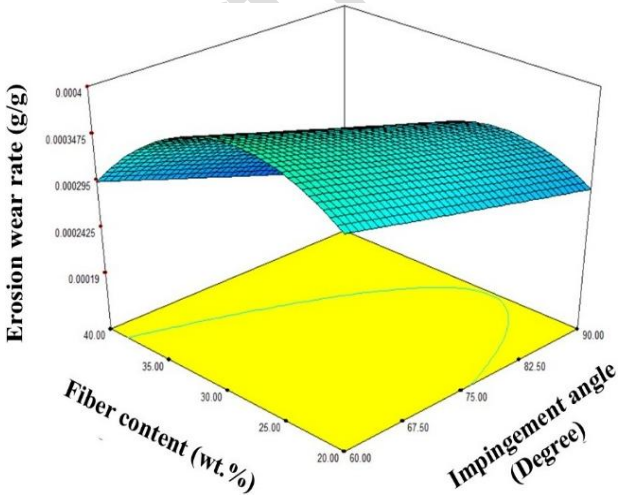

Fig 15c. RSM plot for the response erosion wear rate of F-E composites as a function of impingement angle and fiber content.

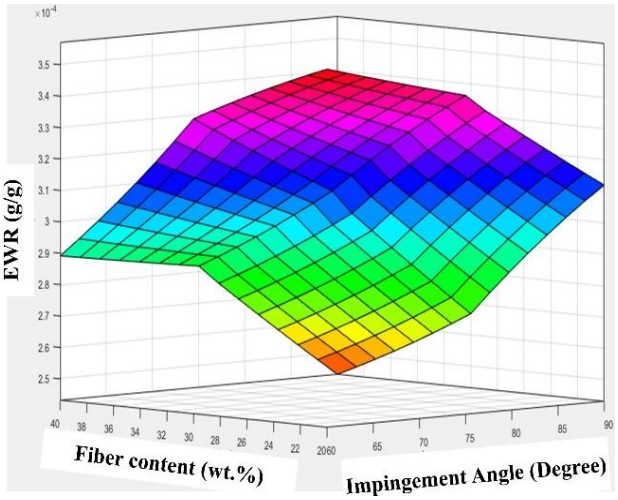

Fig 16c. ANFIS plot for the response erosion wear rate of F-E composites as a function of fiber content and impingement angle.

Modeling of the erosion wear rate of the F-E composites is executed successfully using ANFIS technique and its results is shown in the Table 9. It is evident form the study that, ANFIS model trained under MF "gbellmf" with 500 epochs have given the minimum error of 4.0483×10^{-10} in predicting the erosion wear rate response than other two MFs. Thus, gbellmf based ANFIS model appears to be best and apt for modeling the input factors in understanding the erosion wear rate of F-E composites. Fig.16a-c shows the ANFIS surface plots of the erosion wear rate of the F-E composites for varying input functions. Plots clearly convey the interaction effects of fiber content and impact velocity, impingement angle and impact velocity, fiber content and impingement angle on the output response erosion wear rate. ANFIS plots as similar to the trend noted in RSM are observed here. From the ANFIS three-dimensional plot, it can be inferred that erosion wear rate of the F-E composite is lower for the higher fiber loaded composites (40F-E) when eroded at higher impingement angle impacting with lower velocity.

Table 11. R^2 values of RSM and ANFIS models of F-E composites.

Response	**R-Sq values**	
	RSM model	ANFIS model
Erosion wear rate	0.9827	0.9999

Table 32. Confirmation experiments for validating the experimental values of erosion wear rate in F-E composites using RSM and ANFIS models.

Expt. No	**Model employed**	**Impact velocity (m/s)**	**Impingement angle (Degree)**	**Fiber content (wt. %)**	**EWR (g/g)**
1	Experimental	72	60	40	0.0001961
	RSM	72	60	40	0.0001935
	ANFIS	72	60	40	**0.0001960**
2	Experimental	72	90	20	0.0001983
	RSM	72	90	20	0.0001957
	ANFIS	72	90	20	**0.0001982**
3	Experimental	100	75	30	0.0003100
	RSM	100	75	30	0.0003060
	ANFIS	100	75	30	**0.0003099**

ANOVA results presented in Table 10 clearly explains that the developed regression model for EWR in F-E composite is highly significant with F value 35.50 ($p<0.0001$), which clearly satisfies its suitability for predicting the EWR. Amongst the selected variables, impact velocity ($F=35.50$, $p<0.0001$) is the most significant factors affecting the erosion wear characteristics of F-E composites which clearly reminds the importance of particle kinetic energy is most vital factor governing the material removal. As described before, at higher striking velocities, energy possessed by the erodent particles is sufficient enough to cause the surface damages like, fiber fracture, fiber-matrix debonding, micro cutting, and matrix fracture in F-E composites, thereby paves the way for higher EWR. Second input factor which is reasonably influenced the EWR in F-E composites is impingement angle which shows a mild effect having p value 0.0894 which is supplement to the semi-ductile behavior of the F-E composites, as EWR is maximum at 60° impingement angle, which is simply conveys that such composite materials may also experience both ductile cutting and brittle fracture as coexist. Factor C- fiber content, is least significant factor (with value p=01245) in understanding the erosion wear behavior of the composite materials. However, in terms of quadratic ($p=0.0018$) and interactions ($p=0.0010$), fiber content played a vital role in resisting the erosion wear, particularly at higher fiber loading and operated at higher striking velocities. Optimal fiber loading 40wt. % reinforcement (40F-E) composites showed better EWR, this is owing to the fact that reinforced fiber act as a barrier against the penetration of the particles, also it helps in improving the load bearing the ability of the composites and to some extent, resist matrix removal. Furthermore, interaction between impact velocity and striking

angle (p=0.0330) is significant, which clearly shows that EWR in F-E composites cannot be influenced by impact velocity or impingement angle alone but instead by their combined effect. ANOVA clearly suggested that impact velocity is the main contributing factor for EWR, followed by impingement angle and fiber content. However, fiber loading indirectly influences in enhancing the erosion wears resistance of the F-E composites combined with suitable striking velocity of erodent particles and impingement angles. This work employed two modeling techniques and their efficacy is compared in Table 11. R^2 values of ANFIS and RSM are 0.9999 and 0.9827, respectively, which shows ANFIS has a prediction capability higher than RSM. Furthermore, Comparison among experimental, RSM, and ANFIS values of EWR values are validated by confirmation test and results are indicated in Table 12, which inferred that the experimentally obtained EWR values are in close consistence with predicted ANFIS model than RSM for the range of selected input parameters.

4. WORN SURFACE MORPHOLOGY

The microstructural analysis of the eroded surfaces of F-E composites was studied using FESEM under different magnifications. The major observations such as plastic deformations, crater formations, deep grooves, and micro cracks and cutting are predominant as a result of kinetic energy of the erodent particle carrying while impacting the composite surface. Figure (17a-c) shows FESEM images of the 20F-E composites eroded under impact velocity of 120 m/s at an impingement angle 60°. From the Figur17a-c, crater formation and ploughing with matrix fragmentations is visible. This may be due to the lower fiber content in the 10F-E composite unable to hold the matrix during erosion resulting in crater formation and in turn rise to microcracks or propagation of micro-cutting from the crater side. Moreover, composites with fiber deficient endured localized matrix fragmentations along with the microcracks generation as depicted in the Figure 17c.

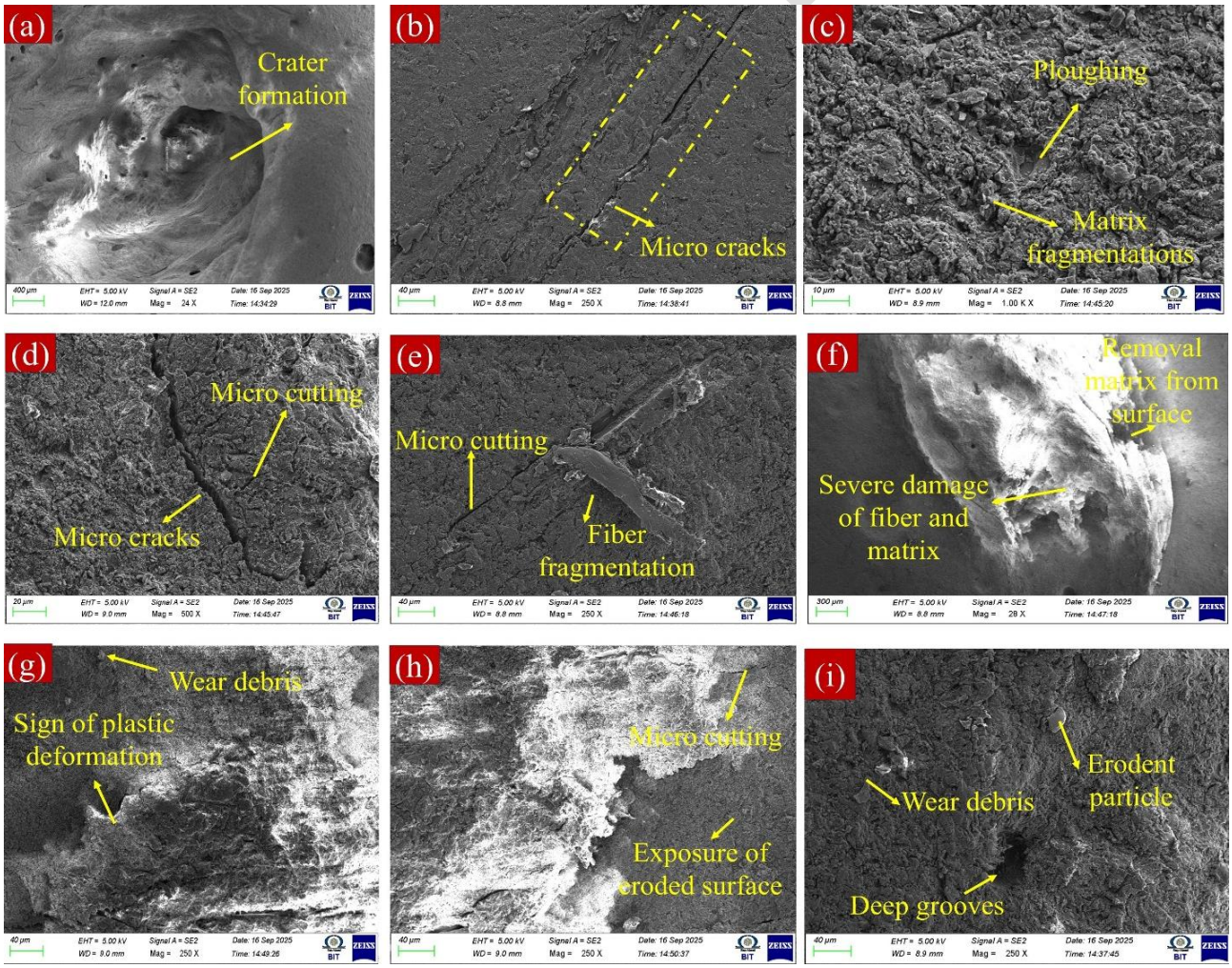

Fig. 17. FESEM images of the eroded surfaces of F-E composites

Figure 17d-f, shows the FESEM images of the 20F-E composites eroded under impact velocity of 120 m/s at an impingement angle 60°. It is evident from the figures that, compared to 20F-E composites, erosion resistance of the 30F-E composites enhanced as incorporated fiber helps in absorbing the energy waves generated due to striking (or erodent) particles. Though fiber content increased, the fiber-matrix damage, and microcracks are inevitable as indicated in the Figure17d-f. This may be aroused due to the insufficient amount of flax fiber to absorb the shocks of the striking particles. Further, addition of 40wt. % of flax fiber, comparatively improved the erosion wear resistance of the 40F-E composites.

The worn surface of the 40F-E composites eroded under the same condition is presented in the Figure17g-i. It is evident the from the micrographs that, micro-cutting, microcracks, and matrix fragmentations have been significantly reduced due to the higher fiber content. This may be owing strong interfacial bonding between fiber and matrix seems to have reduced the erosion wear rate. However, from the Figure17i, crater formation is evident along with the erodent particles embedded on the composite surface. This happens particularly when the composite surface eroded at and impingement angle 60° and 90° as reported earlier [43]. Irrespective of the impact velocity, increased impact angle give rise to the formation of deep grooves accompanying with whirling motion, which may sufficient enough to resist the movement of the alumina particles out from the grooves and resulting in an enlargement of the crater formation along width wise. Figure 18a-b shows micrographs of the 40F-E composite surface embedded with an alumina particle when stroked at an impingement angle 60° and velocity 120 m/s. EDS confirms the presence of alumina articles on the eroded surface with a weight fraction of 5.18%, as shown in the Figure 18b.

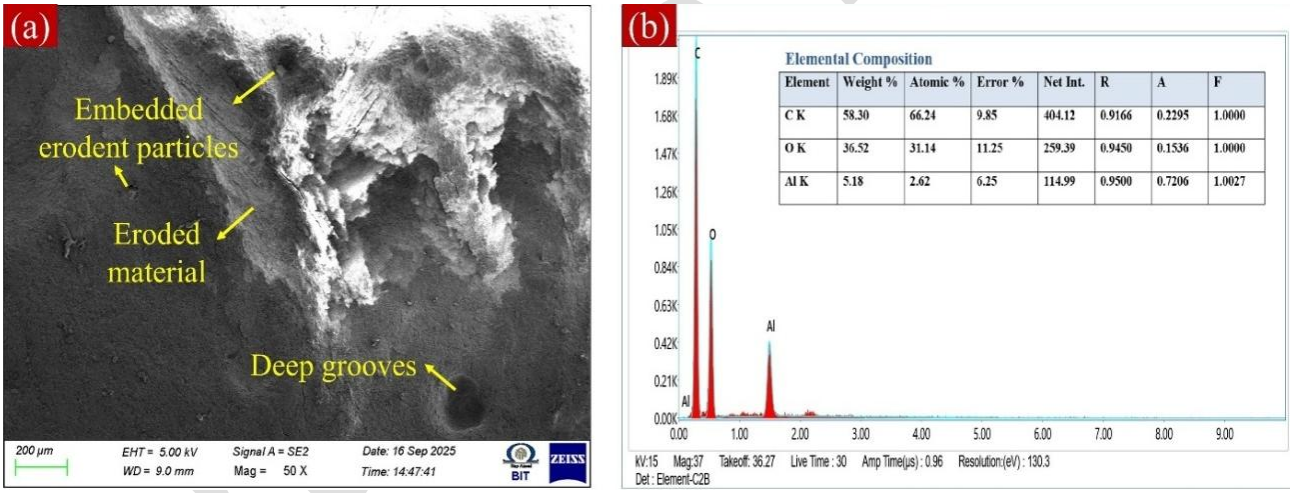

Fig. 18. FESEM of the eroded surfaces with EDS

5. CONCLUSIONS

The following conclusions are drawn:
Results confirms that F-E composites can be employed in tribological applications, such as splash guards, wear strips and guide rails, pump and impeller blades, where the erosion is the main cause of failure, particularly in semi-ductile erosion environment. The 40F-E composite exhibited lowest erosion wear rate of 0.0001654 g/g under the severe condition of impact velocity 72 m/s and impingement angle 90°, while 20F-E and 30F-E showed 0.00019100 g/g and 0.0001983 g/g, respectively. This confirms that increasing fiber content enhances resistance to erosive particle attack by improving load-bearing capacity and reducing matrix removal. The experimental results showed significant effect of test parameters on the erosion wear behaviour of the composites. ANOVA confirms that erosion wear property of the F-E composite is highly influenced by the impact velocity (24.92%), followed by impingement angle and fiber composition. Moreover, erosion nature of the F-E composite is found to be semi-ductile and same was confirmed from the erosion efficiency of the

composites which lies in the range 1.82% to 4.03%. Prediction model developed in ANFIS and RSM found to be beneficial in assessing the wear properties of the composites. Predicting ability of ANFIS with R^2 (0.9999) was more superior than RSM's regression model capability. The same was successfully validated for the experimental results, where ANFIS results were showed closer to experimental ones than RSM. Worn morphology of the samples provides insight into the failure mechanism endured by the composites. Micro-cracks, micro-cutting, partial removal of the fiber-matrix and ploughing are the most dominant wear mechanisms which clearly indicated the semi-ductile behavior of the F-E composites. The present study is focused on a single fiber reinforcement and limited to specific testing conditions, which may not fully represent broad industrial environments. Future studies may emphasis on multi-particle erosion, varying abrasive sizes and temperature and may explore hybrid reinforcement strategies to further improve the erosion wear characteristics of F–E composites.

REFERENCES

[1] S. V. Kumar, K. S. Kumar, H. S. Jailani and G. Rajamurugan, "Mechanical, DMA and sound acoustic behaviour of flax woven fabric reinforced epoxy composites," *Materials Research Express*, vol. 7, no. 8, pp. 085302, 2020, doi: 10.1088/2053-1591/abaea5.

[2] V. K. Shettahalli Mantaiah, "Water absorption behavior and its effect on static mechanical and dynamic mechanical properties of flax fabric reinforced epoxy composites," *Journal of Natural Fibers*, vol. 19, no. 15, pp. 12415–12433, 2022, doi: 10.1080/15440478.2022.2060404.

[3] R. Jeyakumar, S. V. Kumar, J. Rishi and C. Sasikumar, "Mechanical and viscoelastic properties of nanoclay filled bamboo/glass fibre reinforced unsaturated polyester hybrid composites," *Materials Research*, vol. 27, pp. e20230543, 2024, doi: 10.1590/ 1980-5373-MR-2023-0543.

[4] R. Rajiev, S. V. Kumar, H. Singh and E. Sakthivelmurugan, "Multi-response optimization of wear parameters of flax reinforced epoxy composites using Taguchi-GRA-PCA approach," *Indian Journal of Fibre & Textile Research (IJFTR)*, vol. 48, no. 4, pp. 396–408, 2023, doi: 10.56042/ijftr.v48i4.7640

[5] V. K. Shettahalli Mantaiah, S. K. Kallippatti Lakshmanan and S. Kaliappagounder, "Experimental studies on abrasion wear and thermal characteristics of plain derived flax woven fabric reinfsorced epoxy composites," *Journal of Natural Fibers*, vol. 19, no. 15, pp. 10367–10382, 2022, doi: 10.1080/15440478.2021.1993504.

[6] S. V. Kumar and H. Singh, "Wear, morphological and thermal behavior of flax fibre reinforced epoxy composites," *Indian Journal of Fibre & Textile Research (IJFTR)*, vol. 48, no. 3, pp. 326–335, 2023, doi: 10.56042/ijftr.v48i3.6057

[7] E. Sakthivelmurugan, G. Senthil Kumar and S. V. Kumar, "Effect of alkali treatment of Alstonia macrophylla (AS) fiber on dynamic mechanical and machinability properties of polypropylene (PP) composites reinforced with unidirectional AS fiber," *Materials Research*, vol. 26, p. e20230108, 2023, doi: 10.1590/1980-5373-MR-2023-0108.

[8] C. Sasikumar, E. Sakthivelmurugan and J. Rishi, "Effect of salt-water aging on the mechanical properties of flax-woven fabric-reinforced epoxy composites," *Materials and Technology*, vol. 55, no. 6, pp. 851–859, 2021, doi: 10.17222/mit.2021.256.

[9] N. Miyazaki, "Solid particle erosion of composite materials: A critical review," *Journal of Composite Materials*, vol. 50, no. 23, pp. 3175–3217, 2016, doi: 10.1177/0021998315617818

[10] P. Nunthavarawong, C. Chungchoo and P. Niranatlumpong, "Slurry jet erosion wear of particulate polymer composites and metal coating," in *Tribology of Polymer Composites*, Elsevier, 2021, pp. 163–188, doi: 10.1016/B978-0-12-819767-7.00009-8.

[11] I. Finnie, "Erosion of surfaces by solid particles," *Wear*, vol. 3, no. 2, pp. 87–103, 1960, doi: 10.1016/0043-1648(60)90055-7.

[12] J. Bitter, "A study of erosion phenomena part I," *Wear*, vol. 6, no. 1, pp. 5–21, 1963, doi: 10.1016/0043-1648(63)90003-6.

[13] J. Bitter, "A study of erosion phenomena: Part II," *Wear*, vol. 6, no. 3, pp. 169–190, 1963, doi: 10.1016/0043-1648(63)90073-5.

[14] A. Purohit and A. Satapathy, "Erosion wear response of epoxy composites filled with steel industry slag and sludge particles: A comparative study," *IOP Conference Series: Materials Science and Engineering*, vol. 338, no. 1, p. 012059, 2018. doi: 10.1088/1757-899X/338/1/012059.

[15] A. Purohit, A. Satapathy, P. T. Swain, and P. K. Patnaik, "A study on erosion wear behavior of LD sludge reinforced polypropylene composite," *Materials Today: Proceedings*, vol. 18, pp. 4299–4304, 2019. doi: 10.1016/j.matpr.2019.07.388.

[16] P. Pradhan, A. Purohit, I. Mohanty, H. Jena, and B. B. Sahoo, "Erosion wear analysis of coconut shell dust filled epoxy composites using computational fluid dynamics and Taguchi method," *Proceedings of the Institution of Mechanical Engineers, Part C: Journal of Mechanical Engineering Science*, vol. 237, no. 23, pp. 5653–5662, 2023. doi: 10.1177/09544062231167674.

[17] S. Arjula and A. Harsha, "Study of erosion efficiency of polymers and polymer composites," *Polymer Testing*, vol. 25, no. 2, pp. 188–196, 2006, doi: 10.1016/j.polymertesting.2005.10.009.

[18] K. Friedrich, X. Pei and A. Almajid, "Specific erosive wear rate of neat polymer films and various polymer composites," *Journal of Reinforced Plastics and Composites*, vol. 32, no. 9, pp. 631–643, 2013, doi: 10.1177/0731654413478478.

[19] Gupta, A. Kumar, A. Patnaik and S. Biswas, "Effect of different parameters on mechanical and erosion wear behavior of bamboo fiber reinforced epoxy composites," *International Journal of Polymer Science*, vol. 2011, no. 1, p. 592906, 2011, doi: 10.1155/2011/592906.

[20] H. Jena, A. K. Pradhan and M. K. Pandit, "Study of solid particle erosion wear behavior of bamboo fiber reinforced polymer composite with cenosphere filler," *Advances in Polymer Technology*, vol. 37, no. 3, pp. 761–769, 2018, doi: 10.1002/adv.21718.

[21] G. Das and S. Biswas, "Erosion wear behavior of coir fiber-reinforced epoxy composites filled with Al_2O_3 filler," *Journal of Industrial Textiles*, vol. 47, no. 4, pp. 472–488, 2017, doi: 10.1177/1528083716652832.

[22] C. B. Manjunath, C. V. Srinivasa, B. Basavaraju, G. B. Manjunatha, and R. B. Ashok, "A review on tribological behaviour of natural fiber reinforced polymer composites," *IOP Conference Series Materials Science and Engineering*, vol. 925, no. 1, p. 012011, Sep. 2020, doi: 10.1088/1757-899x/925/1/012011.

[23] S. Nayak and J. Mohanty, "Erosion wear behavior of benzoyl chloride modified areca sheath fiber reinforced polymer composites," *Composites Communications*, vol. 18, pp. 19–25, 2020, doi: 10.1016/j.coco.2020.01.006.

[24] P. Sahu and M. Gupta, "Enhancement in erosion wear resistance of sisal composites by eco-friendly treatment and coating," *Materials Research Express*, vol. 6, no. 8, p. 085348, 2019, doi: 10.1088/2053-1591/ab29b5.

[25] J. Sangilimuthukumar *et al.*, "Erosion characteristics of epoxy-based jute, kenaf and banana fibre reinforced hybrid composites," *Materials Today: Proceedings*, vol. 64, pp. 6–10, 2022, doi: 10.1016/j.matpr.2022.03.469.

[26] V. Boggarapu, R. Gujjala and S. Ojha, "A critical review on erosion wear characteristics of polymer matrix composites," *Materials Research Express*, vol. 7, no. 2, p. 022002, 2020, doi: 10.1088/2053-1591/ab6e7b.

[27] R. D. J. Johnson *et al.*, "Erosion performance studies on sansevieria cylindrica reinforced vinylester composite," *Materials Research Express*, vol. 5, no. 3, p. 035309, 2018, doi: 10.1088/2053-1591/aab412.

[28] S. K. Verma *et al.*, "Influence of dolomite on mechanical, physical and erosive wear properties of natural-synthetic fiber reinforced epoxy composites," *Materials Research Express*, vol. 6, no. 12, p. 125704, 2019, doi: 10.1088/2053-1591/ab5abb.

[29] S. Vigneshwaran, M. Uthayakumar and V. Arumugaprabu, "Solid particle erosion study on redmud-an industrial waste reinforced sisal/polyester hybrid composite," *Materials Research Express*, vol. 6, no. 6, p. 065307, 2019, doi: 10.1088/2053-1591/ab0a44.

[30] T. Premkumar *et al.*, "Experimental design and theoretical analysis on the various tribological responses of curauá/polyester composites," *Materials Research Express*, vol. 6, no. 12, p. 125337, 2019, doi: 10.1088/2053-1591/ab5a0b.

[31] P. Antil *et al.*, "Erosion analysis of fiber reinforced epoxy composites," *Materials Research Express*, vol. 6, no. 10, p. 106520, 2019, doi: 10.1088/2053-1591/ab34b4.

[32] S. K. Mahapatra and A. Satapathy, "Analysis and prediction of erosion behavior of epoxy composites using statistical and machine learning techniques," *Proceedings of the Institution of Mechanical Engineers, Part E: Journal of Process Mechanical Engineering*, p. 09544089241233948, 2024, doi: 10.1177/09544089241233948.

[33] R. K. Sharma and S. R. Kumar, "Physicomechanical and erosion wear characterization of PLA/jute fiber biocomposite," *Journal of Elastomers & Plastics*, vol. 56, no. 2, pp. 121–140, 2024, doi: 10.1177/00952443231221263.

[34] E. Gietzen *et al.*, "Experimental investigation of low velocity and high temperature solid particle impact erosion wear," *Wear*, vol. 506–507, p. 204441, 2022, doi: 10.1016/j.wear.2022.204441.

[35] J. Chen *et al.*, "The effect of carbon nanotube orientation on erosive wear resistance of CNT-epoxy based composites," *Carbon*, vol. 73, pp. 421–431, 2014, doi: 10.1016/j.carbon.2014.02.083.

[36] Q. Cheng, M. Li, L. Jiang and Z. Tang, "Bioinspired layered composites based on flattened double-walled carbon nanotubes," *Advanced Materials*, vol. 24, no. 14, pp. 1838–1843, 2012, doi: 10.1002/adma.201200179.

[37] R. K. Sharma, R. K. Das and S. R. Kumar, "Effect of HVOF spraying parameters on fracture, erosion and thermal properties of Fe alloy-based coating materials," *Proceedings of the Institution of Mechanical Engineers, Part L: Journal of Materials: Design and Applications*, vol. 235, no. 7, pp. 1703–1711, 2021, doi: 10.1177/1464420721999682.

[38] S. Kulkarni and Kishore, "Influence of matrix modification on the solid particle erosion of glass/epoxy composites," *Polymers and Polymer Composites*, vol. 9, no. 1, pp. 25–30, 2001, doi: 10.1177/096739110100900103.

[39] S. Rajendran *et al.*, "Solid particle erosion in fibre composites: A review," *Journal of Reinforced Plastics and Composites*, p. 7316844241255007, 2024, doi: 10.1177/07316844241255007.

[40] D. K. Mohapatra, C. R. Deo, P. Mishra and P. Dash, "Effect of pistachio shell particles on mechanical and erosion wear performance of hybrid kenaf/glass polyester composites," *Proceedings of the Institution of Mechanical Engineers, Part J: Journal of Engineering Tribology*, vol. 238, no. 5, pp. 529–544, 2024, do i: 10.1177/13506501231224686

[41] J. R. Mohanty, S. N. Das, H. C. Das, T. K. Mahanta, and S. B. Ghadei,"Solid particle erosion of date palm leaf fiber reinforced polyvinyl alcohol composites,"*Advances in Tribology*, vol. 2014, Article ID 293953, pp. 1–8, 2014. doi: 10.1155/2014/293953.

[42] G. P. Tilly and W. Sage, "The interaction of particle and material behaviour in erosion processes," *Wear*, vol. 16, no. 6, pp. 447–465, 1970, doi: 10.1016/0043-1648(70)90171-7.

[43] S. Pradhan and S. K. Acharya, "Solid particle erosive wear behaviour of Eulaliopsis binata fiber reinforced epoxy composite," Proceedings of the Institution of Mechanical Engineers, Part J: Journal of Engineering Tribology, vol. 235, no. 4, pp. 830–841, 2021, doi: 10.1177/1350650120931645.

[44] V. Prakash, T. Bera and S. K. Acharya, "Mechanical and erosive wear behavior of rubber wood particulate reinforced epoxy composite," Materials Today: Proceedings, vol. 19, pp. 223 227, 2019, doi: 10.1016/j.matpr.2019.06.708.